Journal of Hazardous Materials 177 (2010) 175–182

Contents lists available at ScienceDirect

Journal of Hazardous Materials

journal homepage: www.elsevier.com/locate/jhazmat

Adsorption of volatile organic compounds onto activated carbon cloths derived from a novel regenerated cellulosic precursor

M.E. Ramos[a], P.R. Bonelli[a], A.L. Cukierman[a,b,*], M.M.L. Ribeiro Carrott[c], P.J.M. Carrott[c]

[a] Programa de Investigación y Desarrollo de Fuentes Alternativas de Materias Primas y Energía–PINMATE, Departamento de Industrias, Facultad de Ciencias Exactas y Naturales, Universidad de Buenos Aires, Intendente Güiraldes 2620, Ciudad Universitaria, (C1428BGA) Buenos Aires, Argentina
[b] Cátedra de Farmacotecnia II–Tecnología Especial, Departamento de Tecnología Farmacéutica, Facultad de Farmacia y Bioquímica, Universidad de Buenos Aires, Junín 956, (C1113AAD) Buenos Aires, Argentina
[c] Centro de Química de Évora and Departamento de Química, Colégio Luís António Verney, Universidade de Évora, Rua Romão Ramalho, 59, 7000-671 Évora, Portugal

ARTICLE INFO

Article history:
Received 30 July 2009
Received in revised form 9 November 2009
Accepted 1 December 2009
Available online 11 December 2009

Keywords:
Activated carbon cloths
Microporous materials
Surface properties
Volatile organic compounds adsorption
Electrothermal regeneration

ABSTRACT

Activated carbon cloths (ACC) were prepared from lyocell, a novel regenerated cellulose nanofibre fabric, by phosphoric acid activation in inert atmosphere at two different final thermal treatment temperatures (864 and 963 °C). Benzene, toluene and n-hexane isotherms at 298 and 273 K were measured in order to gain insight into the porous structure of the ACC and to evaluate their performance for the removal of volatile organic compounds (VOCs). The Dubinin–Radushkevich equation was employed to evaluate textural parameters of the ACC. The textural characteristics of the ACC were compared with those previously determined from nitrogen (77 K) and carbon dioxide (273 K) adsorption data. The samples were essentially microporous. The textural parameters calculated from the hydrocarbon isotherms were in good agreement with those evaluated from nitrogen isotherms for the ACC with the wider microporosity. Additionally, the Freundlich model provided a good description of the experimental isotherms for the three volatile organic compounds. The ACC obtained at the higher temperature exhibited a larger adsorption capacity. The ACC were also electrically conductive and showed potential for regeneration by the Joule effect, as determined from macroscopic electrical measurements before and after n-hexane adsorption.

1. Introduction

Volatile organic compounds (VOCs) are present in gas and liquid streams of many industrial applications due to the high production levels. Because they are hazardous to human health and the environment, regulations to control their concentration in effluents are increasingly stringent. Accordingly, continuous research is required to develop more efficient technologies to reduce emissions of these noxious pollutants. Methods such as condensation, absorption, adsorption, catalytic oxidation, and incineration have been employed for abatement of VOCs. Adsorption is by far the most widespread technology applied because it provides an economical way to recover VOCs from a wide range of gaseous streams [1–7].

Activated carbons have been employed for the efficient separation, purification, recovery, and storage of VOCs. Moreover, the use of porous adsorbents to control the amount of hazardous air pollutants can be envisaged not only in the elimination of these species, but also in their monitoring. In the last years, activated carbon cloths (ACC) have been increasingly investigated for this purpose because they offer several technological advantages in comparison with the traditional forms of this widely used porous material. These advantages include faster adsorption kinetics, higher efficiency, and larger capacity for adsorption due to their higher surface area and pore volume. Besides, micropores of the ACC are directly connected to the external surface area, inducing a decrease in the mass transfer resistance that leads to lower pressure drops in flow units [6,8–15]. Furthermore, ACC are essentially microporous materials which are relevant for the adsorption of VOCs in low concentrations in ambient air environments [4,16,17]. Emissions at low concentration levels are quite typical during handling, storage, and distribution of chemicals involving VOCs [3].

In order to develop an adsorption-based separation process, equilibrium data of pure components and textural characterization of the adsorbent are essential [5]. Besides, adsorption of organic compounds with different sizes is a recognized way to character-

* Corresponding author at: Programa de Investigación y Desarrollo de Fuentes Alternativas de Materias Primas y Energía–PINMATE, Departamento de Industrias, Facultad de Ciencias Exactas y Naturales, Universidad de Buenos Aires, Intendente Güiraldes 2620, Ciudad Universitaria, (C1428BGA) Buenos Aires, Argentina.
Tel.: +54 11 45763383; fax: +54 11 45763366.
E-mail address: analea@di.fcen.uba.ar (A.L. Cukierman).

0304-3894/$ – see front matter © 2009 Elsevier B.V. All rights reserved.
doi:10.1016/j.jhazmat.2009.12.014

Nomenclature

A_{BET}	specific surface area BET [$m^2\ g^{-1}$]
E_0	characteristic energy, Dubinin–Radushkevich [$kJ\ mol^{-1}$]
K_F	constant indicative of relative adsorption capacity, Freundlich [$mmol\ g^{-1}\ mbar^{-n}$]
K_L	constant related to the adsorption energy, Langmuir [$mbar^{-1}$]
L_0	mean pore with, Dubinin–Radushkevich [nm]
n	characteristic parameter related to the intensity of adsorption, Freundlich
n_0	micropore capacity [$mmol\ g^{-1}$]
q	volatile compound adsorbed at equilibrium per unit weight of adsorbent [$mmol\ g^{-1}$]
T_0	reference temperature (273 K)
V_m	molar volume [$cm^3\ mol^{-1}$]
X_{mL}	monolayer adsorption capacity, Langmuir [$mmol\ g^{-1}$]

Greek letters

α_0	thermal coefficient at the reference temperature T_0 [K^{-1}]
ν_0	micropore volume, Dubinin–Radushkevich [$cm^3\ g^{-1}$]
ν_S	micropore volume, α_s model [$cm^3\ g^{-1}$]
ν_T	total pore volume [$cm^3\ g^{-1}$]
ρ	electrical resistivity [Ω m]
ρ_0	electrical resistivity at the reference temperature T_0 [Ω m]

ize porous structures of the adsorbents [18]. Regeneration of the spent adsorbents is another critical factor that must be considered in selecting an adsorbent. Desorption by hot gases leads to low concentrations of desorbed vapours. To avoid these inconveniences, "*in situ*" heating by the Joule effect could be an interesting alternative for ACC. They are electrical conductive and, therefore, their regeneration can be carried out by applying an electrical current to the spent adsorbent and using its natural resistance to provide heat. Besides, electrothermal regeneration of the saturated adsorbent can be performed in the same unit in which adsorption occurs [2,3,19–22].

Within this context, the aim of the present work was to investigate the porous texture of activated carbon cloths (ACC) synthesized from lyocell fabric from the adsorption of three different hydrocarbons. Benzene, toluene and n-hexane isotherms were obtained at 298 K and 273 K. The textural characteristics of the ACC as evaluated from these isotherms were compared with those previously determined from nitrogen and carbon dioxide adsorption data. Moreover, conventional two-parameter models were applied to calculate the adsorption capacity of the ACC for their potential use in VOC removal. Finally, the electrical resistivity of the ACC before and after exposure to n-hexane, as model compound, was determined in order to evaluate the feasibility of *in situ* electrothermal regeneration of the saturated adsorbents.

2. Experimental

2.1. Synthesis of activated carbon cloths

Tencel®, a lyocell-based fabric, kindly provided by Santista Textile Group (Buenos Aires, Argentina), was used as precursor for the preparation of the ACC. The elemental composition and some characteristics of the precursor are given in Table 1.

Regenerated cellulosic strips previously weighed were impregnated with H_3PO_4 acid (analytical grade) solutions of 10 wt% concentration at 60 °C overnight. Then, they were dried and weighed. The impregnated samples were thermally treated in a tubular stainless steel reactor of horizontal configuration externally heated by an electric furnace under a N_2 flow (100 mL/min). The activated carbon cloths were heated at 5 °C/min up to two different final temperatures (HTT), 864 and 963 °C. They were labeled as ACC_864 and ACC_963, respectively. Once the desired final temperature was attained, it was held for 1 h. The thermal program included an isothermal step at the initial cellulose decomposition temperature in order to improve mechanical resistance of the ACC. Afterwards, the resulting cloths were cooled under N_2 flow and rinsed thoroughly with distilled hot water until neutral pH. The products were then dried until constant weight. Yields were calculated from weight differences. Details of the experimental procedure have been reported earlier for ACC obtained from other precursors [23,24].

2.2. Characterization of the activated carbon cloths

Porosity development of the ACC was evaluated from the adsorption isotherms of nitrogen at 77 K determined on a CE Instruments Sorptomatic 1990. The ACC were outgassed for 5 h at 423 K under vacuum prior to testing. Narrow microporosity was assessed from the adsorption isotherms of carbon dioxide at 273 K, by using a classical manually operated manometric apparatus. The BET model was employed to evaluate the specific surface area from N_2 isotherms and total pore volumes (ν_T) were estimated from the amount of N_2 adsorbed at the highest relative pressure, near unity. Nitrogen and carbon dioxide isotherms were analyzed by means of the Dubinin–Radushkevich (DR) equation in order to obtain the DR micropore volume (ν_0), characteristic energy (E_0), and the mean pore width (L_0). The latter was estimated from the relationship [25]:

$$L_0 = \frac{10.8}{E_0 - 11.4}$$

The vapour pressure and density of carbon dioxide were taken as 26.126 bar and 1.023 g cm^{-3}, respectively. The value used for the CO_2 affinity coefficient was $\beta = 0.35$. The density of nitrogen was taken as 0.808 g cm^{-3} and the affinity coefficient as $\beta = 0.34$.

2.3. VOC adsorption isotherms

The adsorption isotherms of n-hexane, benzene and toluene at 298 and 273 K were determined gravimetrically using a CI Electronics vacuum microbalance with a DISBAL control unit, with pressure measurement by means of Edwards Barocel 600 capacitance manometers. The temperature was controlled within ±0.1 K using a LTD Grant thermostat. Organic liquids were outgassed by

Table 1
Elemental composition and some characteristics of lyocell precursor.

Sample	Specific mass (gm^{-2})	Warp ($yarn\ cm^{-1}$)	Weft ($yarn\ cm^{-1}$)	N (%)	C (%)	H (%)	O[a] (%)
Tencel®	200	39	24	0.2	42.4	5.9	51.5

[a] Calculated by difference.

Table 2
Vapour pressure, density, affinity coefficient, MW and boiling point of the three adsorbates used.

Adsorbate	Collision diameter[a] (nm)	MW (g mol^{-1})	Density (g cm^{-3})		Saturation pressure (mbar)		β
			298 K	273 K	298 K	273 K	
n-Hexane	0.591 [27]	86.18	0.6563	0.6789	201	60	1.31
Benzene	0.527 [27]	78.11	0.8729	0.8974	127	35	1.00
Toluene	0.665 [28]	92.14	0.8647	0.8872	38	9	1.19

Bird et al. [27], Halpern and Glendening [28].
[a] Calculated from the Lennard–Jones potential energy model.

repeated freeze-thaw cycles. The ACC samples were outgassed at 473 K under vacuum prior to determination of the isotherms. The sensitivity of the weight measurements was 0.01 mg. The adsorption equilibrium for the organic compounds could be reached within 10 min. Total pore volume was calculated as the amount of hydrocarbon adsorbed at the highest relative pressure, using a density calculated from equations recommended in the literature [26]. Vapour pressure, density, affinity coefficient, molecular weight (MW) and collision diameter for the different adsorbates are listed in Table 2.

Textural parameters were calculated from the adsorption isotherms of the organic compounds, applying the DR equation. Moreover, the experimental adsorption equilibrium data for the VOCs on the ACC were fitted to the Langmuir and Freundlich models in order to examine their potential for VOC removal from gaseous effluents. The Langmuir isotherm model is applicable for monolayer adsorption on a homogeneous adsorbent surface with negligible intermolecular forces [29]:

$$q = X_{\mathrm{mL}} \frac{K_{\mathrm{L}} p}{1 + K_{\mathrm{L}} p}$$

where q is the amount of the volatile compound adsorbed per unit weight of adsorbent (mmol g^{-1}), p, the equilibrium pressure (mbar), X_{mL}, the monolayer adsorption capacity (mmol g^{-1}), and K_{L} (mbar^{-1}), a constant related to the adsorption energy. The Freundlich model is widely used for adsorption onto activated carbons with heterogeneous surfaces [29]:

$$q = K_{\mathrm{F}} p^{n}$$

where K_{F} is an empirical constant, indicative of the relative adsorption capacity (mmol g^{-1} mbar^{-n}), and n, a characteristic parameter related to the intensity of adsorption.

2.4. Electrical resistivity of the ACC

Determination of the electrical characteristics of the adsorbents is the preliminary stage to study desorption by the Joule effect. The procedure has been described for other ACC samples [21,23,24]. Briefly, rectangular ACC samples were assembled between two copper electrodes. A standard DC method in a four probe configuration was employed. Measurements were carried out in ambient air and in the warp direction. The temperature at the center of the samples' surface was measured with a copper-constantan thermocouple. The ACC samples were dried during 48 h and the electrical measurements were performed. For each sample, different voltages were applied and the current and temperature were recorded after 5 min. The electrical resistance of the ACC samples was calculated by Ohm's law. The electrical resistivity (ρ) was evaluated accounting for the dimensions of the ACC probe. To evaluate the electrical resistivity parameter (ρ_0) and thermal coefficient (α_0) of the ACC, a decreasing linear dependence of the resistivity on the temperature was applied to fit the experimental data. It is given by

$$\frac{\rho}{\rho_0} = 1 + \alpha_0 (T - T_0)$$

where ρ is the electrical resistivity (Ω m) at the temperature of the activated carbon cloth surface (T), ρ_0, the electrical resistivity (Ω m) at the reference temperature T_0 (273 K), and α_0, the thermal coefficient (K^{-1}) at the reference temperature T_0.

In order to evaluate the feasibility of regenerating the ACC loaded with VOCs by the Joule effect, macroscopic measurements of the electrical resistance of the ACC after n-hexane adsorption were also carried out. For this purpose, ACC were exposed in n-hexane saturated ambient for 48 h, in order to reach saturation capacity. Finally, the electrical resistivity of the ACC loaded with n-hexane was determined following the procedure described above.

3. Results and discussion

Nitrogen adsorption/desorption isotherms for the ACC have been previously reported [30]. They exhibited a typical type I isotherm according to the IUPAC classification, which is indicative of essentially microporous materials, and were reversible [23,24]. The ACC developed at the higher temperature presented a larger N_2 adsorption capacity and a higher mean pore width.

Yield and textural parameters calculated from the nitrogen and carbon dioxide isotherms are summarized in Table 3. The results in the table indicate that increasing the HTT induced a decrease in ACC yield due to a larger release of volatile compounds during thermal treatment [23,24] which is favoured at the higher temperature. The derived ACC presented high surface areas and total pore volumes. Higher activation temperature led to a larger adsorption capacity and a wider microporosity development. Specific surface area (A_{BET}), micropore volume, $v_0(N_2)$, and the mean pore width increase with activation degree. Increasing the final temperature also promotes widening of micropores and changes in the pore size distribution, as inferred from comparison of the values of $v_0(CO_2)$ and $v_0(N_2)$. As may be noticed, the former remained almost constant, while the latter increased. The lower values of $L_0(CO_2)$ in comparison with $L_0(N_2)$ for these samples is also an indication of the presence of some wider microporosity.

Table 3
Yield and textural characteristics obtained by application of the DR and BET methods to N_2 and CO_2 adsorption isotherms determined for the lyocell-derived activated carbon cloths.

Sample	Yield (%)	Nitrogen					Carbon dioxide		
		v_{T} (cm^3 g^{-1})	A_{BET} (m^2 g^{-1})	v_0 (cm^3 g^{-1})	E_0 (kJ mol^{-1})	L_0 (nm)	v_0 (cm^3 g^{-1})	E_0 (kJ mol^{-1})	L_0 (nm)
ACC_963	19.8	0.67	1705	0.64	21.3	1.09	0.41	24.3	0.84
ACC_864	26.9	0.52	1229	0.48	24.2	0.84	0.45	25.9	0.75

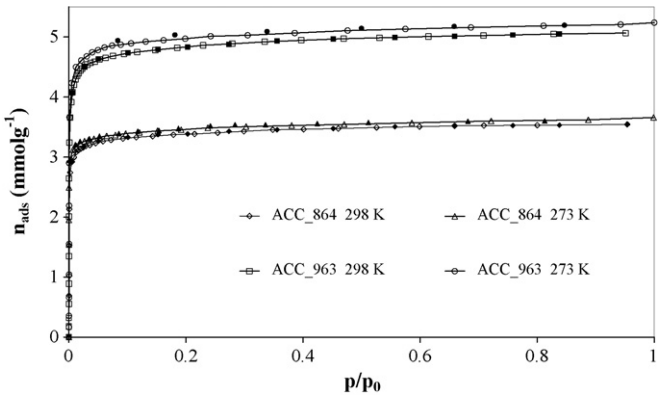

Fig. 1. Hexane adsorption/desorption isotherms obtained at 298 and 273 K for the ACC developed at the two different temperatures. Open symbols: adsorption; filled symbols: desorption.

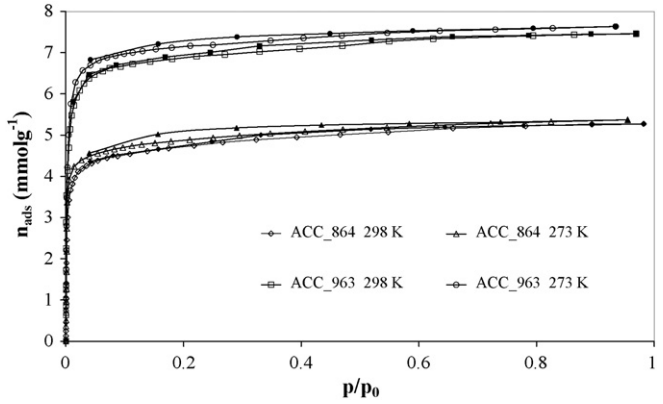

Fig. 2. Benzene adsorption/desorption isotherms obtained at 298 and 273 K for the ACC developed at the two different temperatures. Open symbols: adsorption; filled symbols: desorption.

Hexane, benzene and toluene adsorption isotherms obtained at 298 and 273 K for the two ACC samples are depicted in Figs. 1–3. All the isotherms (Figs. 1–3) showed a plateau over a wide range of relative pressures which is characteristic of microporous materials, in agreement with nitrogen adsorption data [30]. For the sample obtained at the higher final temperature, there is an opening of the knee which points to a widening of microporosity with the degree of activation. A larger specific surface area resulted in a higher adsorption capacity of the different adsorbates employed over the whole experimental range. As expected, the uptake of each organic compound increased at the lower temperature employed for isotherm determination, since adsorption is an exothermic process and the system is in equilibrium. Mean pore radii were higher than the molecular size of the adsorbates, as estimated from the

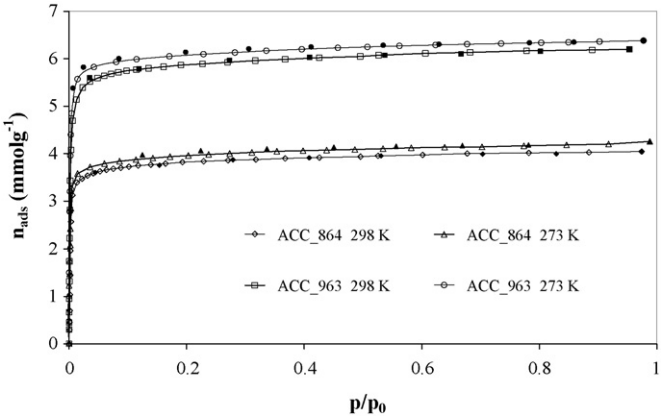

Fig. 3. Toluene adsorption/desorption isotherms obtained at 298 and 273 K for the ACC developed at the two different temperatures. Open symbols: adsorption; filled symbols: desorption.

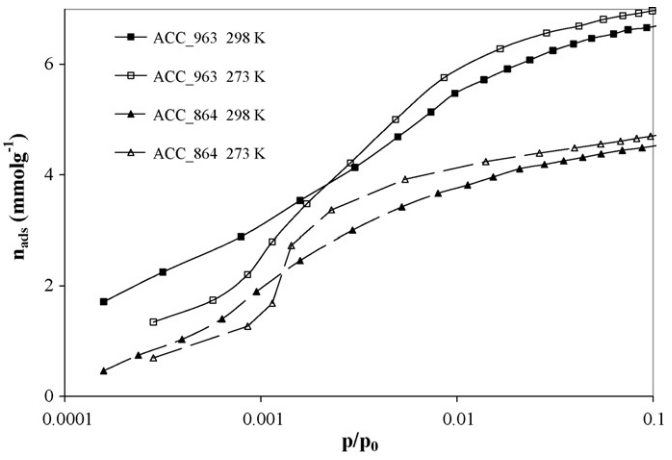

Fig. 4. Benzene adsorption isotherms at low relative pressures for the ACC obtained at the two different temperatures.

Table 4
Textural parameters of the lyocell-derived ACC as calculated from adsorption isotherms of the different organic molecules.

	ACC_963		ACC_864	
	298	273	298	273
n-hexane				
v_T (cm^3 g^{-1})	0.66	0.66	0.46	0.46
v_0 (cm^3 g^{-1})	0.63	0.63	0.40	0.39
E_0 (kJ mol^{-1})	22.9	23.0	24.8	24.6
L_0 (nm)	0.94	0.93	0.81	0.82
Benzene				
v_T (cm^3 g^{-1})	0.67	0.66	0.47	0.47
v_0 (cm^3 g^{-1})	0.64	0.64	0.42	0.43
E_0 (kJ mol^{-1})	23.1	24.0	24.7	25.5
L_0 (nm)	0.92	0.86	0.81	0.77
Toluene				
v_T (cm^3 g^{-1})	0.66	0.66	0.43	0.44
v_0 (cm^3 g^{-1})	0.64	0.64	0.41	0.41
E_0 (kJ mol^{-1})	23.3	23.6	24.4	24.7
L_0 (nm)	0.91	0.88	0.83	0.81

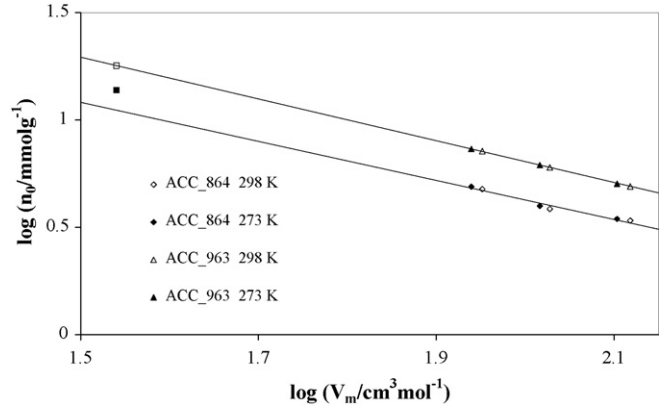

Fig. 5. Log–log plot for the two ACC employed for all the organic adsorbates. Values corresponding to adsorption of nitrogen (77 K) are included (□, ACC_963; ■, ACC_864).

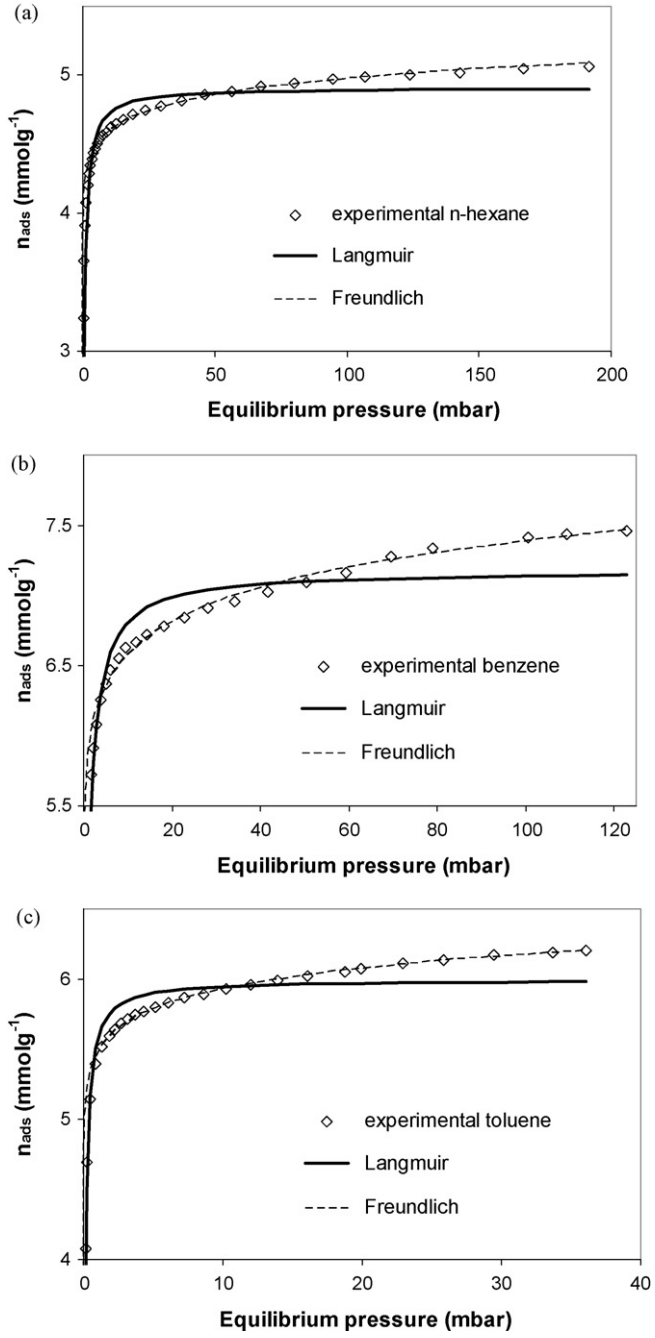

Fig. 6. Comparison between experimental and predicted VOCs adsorption isotherms at 298 K for the ACC_963: (a) n-hexane; (b) benzene; (c) toluene.

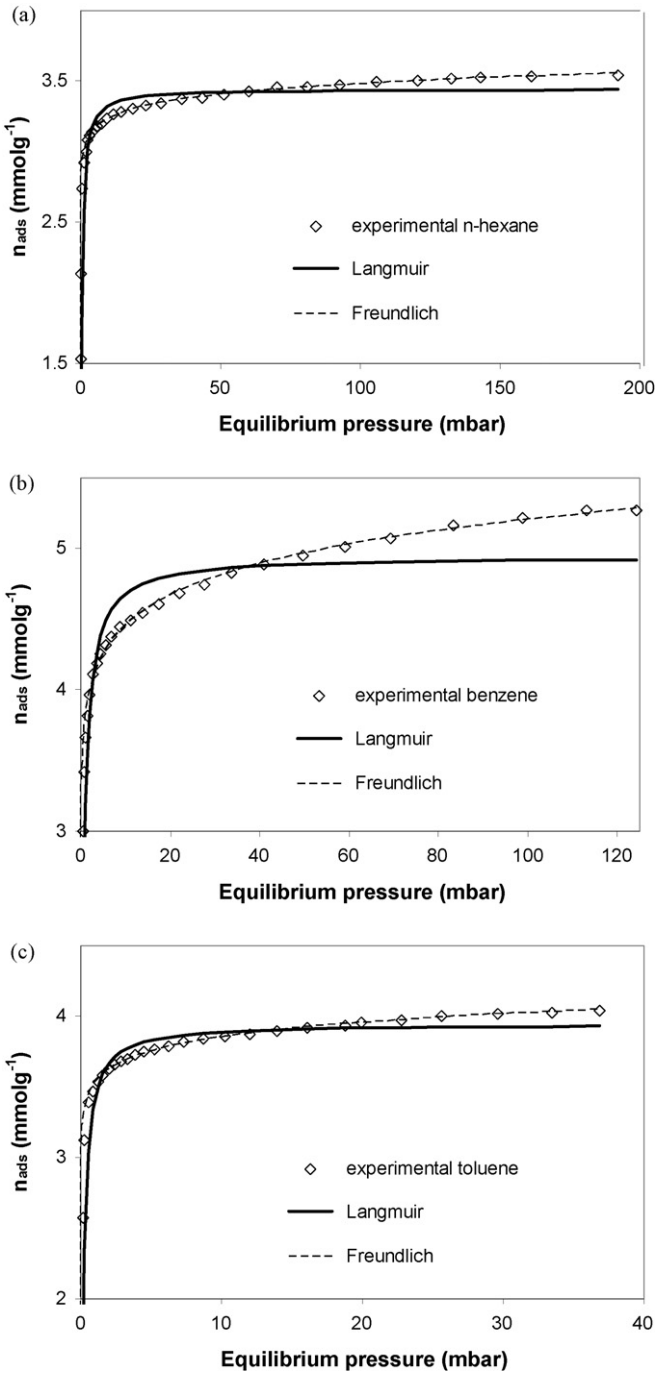

Fig. 7. Comparison between experimental and predicted VOCs adsorption isotherms at 298 K for the ACC_864: (a) n-hexane; (b) benzene; (c) toluene.

collision diameter, pointing to negligible activated entry effects (Tables 2 and 3).

The benzene isotherms (Fig. 2) presented a hysteresis loop, characteristic of slit-shaped pores of size close to the minimum molecular dimension of the adsorbate [31,32]. This loop becomes wider and shifts to lower relative pressures for the isotherms determined at 273 K. In order to better observe the differences in the data at the lower p/p_0 region, Fig. 4 shows the benzene adsorption isotherms, expressing the relative pressure p/p_0 in a logarithmic form.

The results show that, for the two ACC, the adsorption capacity of benzene at high relative pressures was higher than for the other organic compounds (Figs. 1–3). At low relative pressures, adsorption affinity was dependent on the temperature of the isotherm and on the porous material. With regard to benzene adsorption in the low pressure region ($p/p_0 < 2 \times 10^{-3}$), the uptake was higher at the higher temperature used (Fig. 4). The trend may possibly be related to constrictions in pore entrances and pore shape. Benzene is a disc-like molecule which is different from the molecular structure of the other compounds. The rise in temperature seemed to facilitate the diffusion of benzene molecules through narrow constrictions, thus enhancing the adsorption capacity at low relative pressure [33].

The adsorption isotherms of the organic compounds were satisfactorily represented by the DR equation ($R^2 > 0.99$). The range of relative pressures considered for data fitting was 0.01–0.1 for all the samples. The parameters v_0, E_0, L_0, and the total pore volume (v_T)

Table 5
Estimated parameter values of the Langmuir and Freundlich models for VOC adsorption onto ACCs.

			ACC_963		ACC_864	
			273 K	298 K	273 K	298 K
n-Hexane	*Langmuir*	X_{mL} (mmol g^{-1})	5.11	4.91	3.56	3.44
		K_L (mbar^{-1})	5.57	2.57	5.21	2.87
		R^2	0.944	0.857	0.734	0.687
	Freundlich	K_F (mmol g^{-1} mbar^{-n})	4.62	4.25	3.21	3.01
		n	0.029	0.034	0.030	0.032
		R^2	0.999	0.995	0.995	0.998
Benzene	*Langmuir*	X_{mL} (mmol g^{-1})	7.45	7.17	5.09	4.94
		K_L (mbar^{-1})	5.64	1.85	6.80	1.77
		R^2	0.970	0.923	0.887	0.877
	Freundlich	K_F (mmol g^{-1} mbar^{-n})	6.61	5.86	4.39	3.81
		n	0.04	0.05	0.06	0.07
		R^2	0.999	0.996	0.999	0.996
Toluene	*Langmuir*	X_{mL} (mmol g^{-1})	6.23	5.99	4.09	3.95
		K_L (mbar^{-1})	79.54	12.76	39.6	6.6
		R^2	0.988	0.975	0.984	0.900
	Freundlich	K_F (mmol g^{-1} mbar^{-n})	5.98	5.47	3.87	3.53
		n	0.029	0.035	0.039	0.038
		R^2	1.000	1.000	1.000	0.999

calculated from the adsorption at the maximum relative pressure, are listed in Table 4.

As can be seen in Table 4, the micropore volumes obtained for the different organic adsorbates agree within the limits of experimental error. The temperature used for the isotherm determinations did not exert by itself a strong influence on the textural parameters. The E_0 values suggested the existence of a stronger adsorbate–adsorbent interaction in the ACC having narrower pores [32,34]. In the case of ACC_864, the nitrogen volume adsorbed near saturation was on average 10% higher than the total volume obtained by using the organics as adsorbates, likely due to constrictions in some pore entrances. This effect could not be attributed only to an influence of the lower temperature used for nitrogen adsorption, since the total pore volume of the sample ACC_963 is almost identical for all the adsorbates employed and very similar to those obtained with nitrogen. Otherwise the higher micropore volume given by N_2 in comparison with the values obtained for the organic adsorbates could indicate that the density of N_2 may be higher than the normal liquid density in narrower pores [35] or that the nitrogen molecule adapts rapidly to the shape of the pore entrance [36].

Fig. 5 shows a log–log relationship between the micropore capacity of each ACC (n_0/mmol g^{-1}) and the molar volume of the adsorbate at the isotherm temperature (V_m/cm^3 mol^{-1}). It can be seen in Fig. 5 that there was a linear relationship between log(n_0) and log(V_m) in agreement with other reported results [36]. In drawing the lines, the points corresponding to nitrogen adsorption were not considered. The ACC_963 showed a closer behaviour to the Gurvitsch rule, showing a slope near unity (0.98). It indicates that the quantity adsorbed by a porous material is independent of the adsorbate [4]. For those adsorbents, the amount adsorbed at high pressures is independent of the nature of the adsorbate. It could be related with a wider microporosity. On the other hand, the nitrogen value did not agree with the other adsorbates in the case of ACC_864, and the slope was less than unity (slope ~0.90) which could be associated with the presence of constrictions in pore entrances [36].

The adsorption isotherms obtained at 298 K and predictions of the Langmuir and Freundlich models are shown in Figs. 6 and 7(a–c). The corresponding characteristic parameters of the models along with the correlation coefficients are given in Table 5.

Table 6
Adsorption capacity of different carbon-based adsorbents.

Authors	Adsorbate	Adsorbent	S_{BET} (m^2 g^{-1})	v_T (ml g^{-1})	v_0 (ml g^{-1})	Adsorption capacity (mmol g^{-1})	
						DR	Freundlich
Oh et al. [16]	Toluene	Activated carbon nanofibers	1403	0.65	0.505	7.0	–
Cardoso et al. [8]	n-Hexane	Activated carbon	1336	na	0.56	4.4	–
Ramirez et al. [39]	Benzene	Activated carbon fibres	1604	na	0.73	8.1	–
Singh et al. [6]	n-Hexane	Activated carbon fabric	1565	0.65	na	–	1.3
	Benzene					–	0.7
Huang et al. [40]	Benzene	Activated carbon fibers	1680	na	0.43	8.3	–
Benkhedda et al. [41]	Toluene	Activated carbon	1300	na	na	–	2.4
Cal et al. [15]	Benzene	Activated carbon cloth	1330	0.694	na	7.8	–
			1860	1.023	na	6.2	–
Present work	n-Hexane	ACC-864	1229	0.52	0.48	3.1	3.0
		ACC-963	1705	0.67	0.64	4.8	4.3
	Benzene	ACC-864	1229	0.52	0.48	4.7	3.8
		ACC-963	1705	0.67	0.64	7.2	5.9
	Toluene	ACC-864	1229	0.52	0.48	3.9	3.5
		ACC-963	1705	0.67	0.64	6.0	5.5

na, not available.

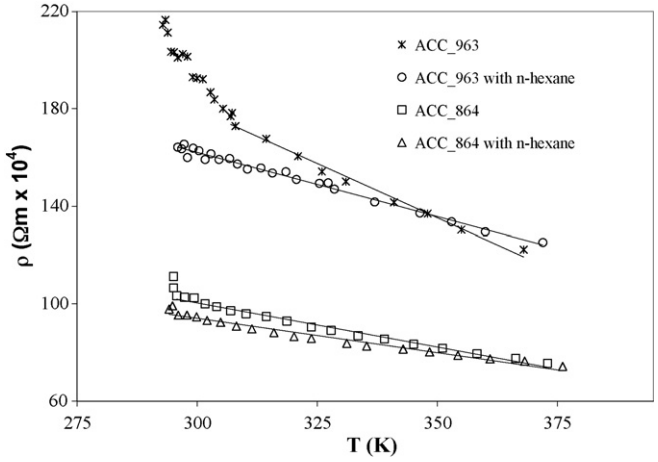

Fig. 8. Electrical resistivity as a function of the surface central temperature for the ACC obtained at the two different final temperatures before and after n-hexane exposure.

As inferred from Figs. 6 and 7, the Freundlich adsorption isotherm satisfactorily described the experimental data, while the Langmuir model failed to represent the results over the whole range of pressures. The observations agree with the higher R^2 values obtained for the former (Table 5). The Langmuir equation gives a good fit at the low pressure range; it is attributed to low interactions between the molecules due to low surface coverage [5].

The parameters related with the adsorption capacity of ACC_963 at the two temperatures were higher than those obtained for the ACC_864 (X_{mL} and K_F, Table 5). Accordingly, ACC_963 would be more efficient for VOC removal from gaseous effluents. With respect to the adsorption of the different organic compounds onto each ACC, X_{mL} and K_F values were higher for the adsorption at 273 K. Among the adsorbates tested, benzene exhibited the highest relative adsorption capacity (K_F, Table 5), while n-hexane showed the minimum K_F value. This trend could be related to dispersive π–π interactions between the aromatic compounds and the π system of pseudographitic planes of the ACC [37]. On the other hand, it has been shown that flat molecules are better adsorbed between the basic planes of the activated carbons. The shape and size of benzene allow an easier diffusion in the narrow ultramicropores of ACC [14,38].

Meaningful direct comparisons with results of adsorption capacity of different carbon materials published in the literature are difficult due to different experimental conditions employed. Nevertheless, taking into account reported isotherms measured under quite similar experimental conditions to those employed in the present work, adsorption capacity values estimated according to Freundlich or DR equations are presented as an approach in Table 6. As may be appreciated, the adsorption capacity values of the developed ACC were comparable to those obtained for other carbon-based adsorbents.

Fig. 8 shows values of the electrical resistivity (ρ) as a function of the central temperature measured at the surface of the ACC obtained at the two different final temperatures, before and after n-hexane adsorption. The characteristic parameters, ρ_0 and α_0, as obtained by linear regression analysis with high correlation coefficients ($R^2 \geq 0.98$), are reported in Table 7.

It can be seen from Fig. 8 that the ACC obtained at the two different temperatures, before and after n-hexane exposure, were electrically conductive, showing a semiconductor behaviour. Comparison of the electrical behaviour of the ACC samples before n-hexane adsorption indicates that increasing the final thermal treatment temperature-induced decreases in ρ_0. It may be attributed to porosity development which could cause discontinuous jumps in the electrical flow and reduction of the effective cross-section.

Table 7
Electrical resistivity (ρ_0) and thermal coefficient (α_0) of the lyocell-derived ACC before and after n-hexane adsorption.

ACC	$\alpha_0 \times 10^3$ (K^{-1})	$\rho_0 \times 10^3$ (Ω m)
ACC_963	−4.5	20.7
ACC_963_l[a]	−3.0	17.6
ACC_864	−3.3	11.0
ACC_864_l[a]	−2.8	10.2

[a] Sample saturated with n-hexane.

The adsorption of n-hexane onto both ACC reduced the electrical resistivity and the thermal coefficient of the samples (Fig. 8, Table 7). The ACC_963 showed a greater reduction of the electrical parameters, probably due to the higher amount of n-hexane adsorbed on this sample. This behaviour was also observed for activated carbon monoliths at different uniform loadings with toluene [2]. For these samples, resistivity seemed to decrease as the loading increased. Electrical conductivity in semiconductors depends on the creation of positive holes in the valence band due to the promotion of an electron to the conduction band. Adsorbed molecules could interact with electrons and reduce their mobility. This phenomenon would decrease recombination processes and increase the number of holes, thus enhancing the conductivity [2].

Additionally, all the samples were heated by the Joule effect, being the range of measured temperatures comprised between 300 and 400 K for voltages between 10 and 20 V. The ACC showed a rapid rate of heating. Different central surface temperatures were achieved in a very short time (less than 30 s). The ACC pre-saturated with n-hexane were weighed before and after the electrical measurements. The samples presented a high level of regeneration (95.6% for ACC_864 and 97.5% for ACC_963) without appreciable changes in surface properties. Accordingly, the heat generated has potential for *in situ* regeneration of the ACC loaded with VOCs and for recovery of these compounds.

4. Conclusions

Adsorption isotherms of n-hexane, benzene and toluene onto activated carbon cloths developed from a novel fabric precursor at two different final thermal treatment temperatures were measured. The isotherms of the three VOCs exhibited a classical type-I shape, characteristic of microporous adsorbents. The textural parameters calculated from the hydrocarbon isotherms by applying the Dubinin–Radushkevich model were in good agreement with those evaluated from nitrogen isotherms for the ACC with the wider microporosity. Experimental adsorption data for all the volatile organic compounds employed were also satisfactorily fitted to the Freundlich model over the whole equilibrium pressure range. The adsorption capacity of the ACC obtained at 964 °C was 1.5 times higher than those developed at 864 °C. This result is attributed to the higher specific surface area, average pore diameter and large micropore volume shown by the former. Moreover, the electrical behavior of the ACC indicated that they have great potential for electrical applications and, particularly, for *in situ* regeneration of the spent adsorbents after being used for VOC removal by the Joule effect.

Acknowledgements

Financial support from Consejo Nacional de Investigaciones Científicas y Técnicas (CONICET), Universidad de Buenos Aires (UBA), and Agencia Nacional de Promoción Científica y Tecnológica (ANPCYT–FONCYT) from Argentina is gratefully acknowledged. The

authors also express their thanks to the EUROPEAID Co-operation Office - Alfa Programme (Project ALFA II 0412 FA FI).

References

[1] N. Mohan, G.K. Kannan, S. Upendra, R. Subha, N.S. Kumar, Breakthrough of toluene vapours in granular activated carbon filled packed bed reactor, J. Hazard. Mater. 168 (2009) 777–781.
[2] F.D. Yu, L. Luo, G. Grevillot, Electrothermal swing adsorption of toluene on an activated carbon monolith. Experiments and parametric theoretical study, Chem. Eng. Process. 46 (2007) 70–81.
[3] D. Das, V. Gaur, N. Verma, Removal of volatile organic compound by activated carbon fiber, Carbon 42 (2004) 2949–2962.
[4] A.B. Fuertes, G. Marbán, D.M. Nevskaia, Adsorption of volatile organic compounds by means of activated carbon fibre-based monoliths, Carbon 41 (2003) 87–96.
[5] F.D. Yu, L.A. Luo, G. Grevillot, Adsorption isotherms of VOCs onto an activated carbon monolith: experimental measurement and correlation with different models, J. Chem. Eng. Data 47 (2002) 467–473.
[6] K.P. Singh, D. Mohan, G.S. Tandon, G.S.D. Gupta, Vapor-phase adsorption of hexane and benzene on activated carbon fabric cloth: equilibria and rate studies, Ind. Eng. Chem. Res. 41 (2002) 2480–2486.
[7] W.-T. Tsai, C.-Y. Chang, C.-Y. Ho, L.-Y. Chen, Adsorption properties and breakthrough model of 1,1-dichloro-1-fluoroethane on activated carbons, J. Hazard. Mater. 69 (1999) 53–66.
[8] B. Cardoso, A.S. Mestre, A.P. Carvalho, J. Pires, Activated carbon derived from cork powder waste by KOH activation: preparation, characterization and VOCs adsorption, Ind. Eng. Chem. Res. 47 (2008) 5841–5846.
[9] A. Linares-Solano, D. Cazorla-Amorós, Adsorption on activated carbon fibers, in: E.J. Bottani, J.M.D. Tascón (Eds.), Adsorption by Carbons, Elsevier, Oxford, UK, 2008, pp. 431–449.
[10] J.M.D. Tascón, Overview of carbon materials in relation to adsorption, in: E.J. Bottani y, J.M.D. Tascón (Eds.), Adsorption by Carbons, Elsevier, Oxford, UK, 2008, pp. 15–49.
[11] C.-C. Wang, C.-C. Hu, Electrochemical catalytic modification of activated carbon fabrics by ruthenium chloride for supercapacitors, Carbon 43 (2005) 1926–1935.
[12] F. Rodríguez-Reinoso, Carbons, in: F. Schüth, K.S.W. Sing, J. Weitkamp (Eds.), Handbook of Porous Solids, Wiley VCH, Weinheim, 2002, pp. 1766–1827.
[13] P.J.M. Carrott, J.M.V. Nabais, M.M.L. Ribeiro Carrott, J.A. Pajares, Preparation of activated carbon fibres from acrylic textile fibres, Carbon 39 (2001) 1543–1555.
[14] C. Brasquet, P. Le Cloirec, Effects of activated carbon cloths surface on organic adsorption in aqueous solutions. Use of statistical methods to describe mechanisms, Langmuir 15 (1999) 5906–5912.
[15] M.P. Cal, M.J. Rood, S.M. Larson, Gas phase adsorption of volatile organic compounds and water vapor en activated carbon cloth, Enfuem 11 (1997) 311–315.
[16] G.-Y. Oh, Y.-W. Ju, M.-Y. Kim, H.-R. Jung, H.-J. Kim, W.-J. Lee, Adsorption of toluene on carbon nanofibers prepared by electrospinning, Sci. Tot. Environ. 393 (2008) 341–347.
[17] X. Hu, S. Qiao, X.S. Zhao, G.Q. Lu, Adsoprtion study of benzene in ink-bottle-like MCM-41, Ind. Eng. Chem. Res. 40 (2001) 862–867.
[18] F. Blanco, X. Vilanova, V. Fierro, A. Celzard, P. Ivanov, E. Llobet, N. Cañellas, J.L. Ramírez, X. Correig, Fabrication and characterization of microporous activated carbon-based pre-concentrators for benzene vapours, Sens. Actuators 132 (2008) 90–98.
[19] P.D. Sullivan, M.J. Rood, G. Grevillot, J.D. Wander, J.K. Hay, Activated carbon fiber cloth electrothermal swing adsorption system, Environ. Sci. Technol. 38 (2004) 4865–4877.
[20] A. Subrenat, J. Bellettre, P. Le Cloirec, 3-D numerical simulations of flows in a cylindrical pleated filter packed with activated carbon cloth, Chem. Eng. Sci. 58 (2003) 4965–4973.
[21] A. Subrenat, J.N. Baléo, P. Le Cloirec, P.E. Blanc, Electrical behaviour of activated carbon cloth heated by the Joule effect: desorption application, Carbon 39 (2001) 707–716.
[22] J.D. Snyder, J.G. Leesch, Methyl bromide recovery on activated carbon with repeated adsorption and electrothermal regeneration, Ind. Eng. Chem. Res. 40 (2001) 2925–2933.
[23] M.E. Ramos, P.R. Bonelli, A.L. Cukierman, Physico-chemical and electrical properties of activated carbon cloths. Effect of inherent nature of the fabric precursor, Colloids Surf. A 32 (2008) 86–92.
[24] M.E. Ramos, J.D. González, P.R. Bonelli, A.L. Cukierman, Effect of process conditions on physicochemical and electrical characteristics of denim-based activated carbon cloths, Ind. Eng. Chem. Res. 46 (2007) 1167–1173.
[25] H.F. Stoeckli, P. Rebstein, L. Ballerini, On the assessment of microporosity in active carbons, a comparison of theoretical and experimental data, Carbon 28 (1990) 907–909.
[26] R.C. Reid, J.M. Prausnitz, B.E. Poling, The Properties of Gases and Liquids, McGraw-Hill, New York, 1986.
[27] R.B. Bird, W.E. Stewart, E.N. Lightfoot, Fenómenos de transporte, Editorial Reverté, Barcelona, 1964.
[28] A.M. Halpern, E.D. Glendening, Estimating molecular collision diameters using computational methods, J. Mol. Struct. (Theochem.) 365 (1996) 9–12.
[29] D.D. Do, Adsorption Analysis: Equilibria and Kinetics, Imperial College Press, London, 1998.
[30] M.E. Ramos, P.R. Bonelli, A.L. Cukierman, M.M.L. Ribeiro Carrott, P.J.M. Carrott, Influence of thermal treatment conditions on porosity development and mechanical properties of activated carbon cloths from a novel nanofibre-made fabric, Mater. Chem. Phys. 116 (2009) 310–314.
[31] C. Moreno-Castilla, J. Rivera-Utrilla, F. Carrasco-Marín, M.V. López-Ramón, On the carbon dioxide and benzene adsorption on activated carbons to study their micropore structure, Langmuir 13 (1997) 5208–5210.
[32] P.J.M. Carrott, M.M.L. Ribeiro Carrott, I.P.P. Cansado, J.M.V. Nabais, Reference data for the adsorption of benzene on carbon materials, Carbon 38 (2000) 465–474.
[33] Y.-C. Chiang, P.-C. Chiang, C.-P. Huang, Effects of pore structure and temperature on VOC adsorption on activated carbon, Carbon 39 (2001) 523–534.
[34] P.J.M. Carrott, I.P.P. Cansado, M.M.L. Ribeiro Carrott, On the L_0/σ range of the TVFM, Adsorpt. Sci. Technol. 4 (2006) 205–213.
[35] M.M.L. Ribeiro Carrott, A.J.E. Candeias, P.J.M. Carrott, P.I. Ravikovitch, A.V. Neimark, A.D. Sequeira, Adsorption of nitrogen, neopentane, n-hexane, benzene and methanol for the evaluation of pore sizes in silica grades of MCM-41, Micropor. Mesopor. Mater. 47 (2001) 323–337.
[36] P.J.M. Carrott, Molecular sieve behaviour of activated carbons, Carbon 33 (1995) 1307–1312.
[37] E. Díaz, S. Ordóñez, A. Vega, Adsorption of volatile organic compounds onto carbon nanotubes, carbon nanofibers, and high-surface-area graphites, J. Colloid Interface Sci. 305 (2007) 7–16.
[38] N.A. Gregg, K.S.W. Sing, Adsorption Surface Area and Porosity, 2nd ed., Academic Press, London, 1982.
[39] D. Ramirez, S. Qi, M.J. Rood, Equilibrium and heat of adsorption for organic vapors and activated carbons, Environ. Sci. Technol. 39 (2005) 5864–5871.
[40] Z.-H. Huang, F. Kang, Y.-P. Zheng, J.-B. Yang, K.-M. Liang, A desorption of trace polar methy-ethyl-ketone and non-polar benzene vapors on viscose rayon-based activated carbon fibers, Carbon 40 (2002) 1363–1367.
[41] J. Benkhedda, J.-N. Jaubert, D. Barth, Experimental and modeled results describing the adsorption of toluene onto activated carbon, J. Chem. Eng. Data 45 (2000) 650–653.